

# Quantification of magnetic force microscopy using a micronscale current ring

Linshu Kong<sup>a)</sup> and Stephen Y. Chou

Department of Electrical Engineering, NanoStructure Laboratory, University of Minnesota, Minneapolis, Minnesota 55455

(Received 13 March 1996; accepted for publication 13 February 1997)

Metal rings with inner diameters of 1 and 5  $\mu\text{m}$ , fabricated using electron-beam lithography, were used to calibrate magnetic force microscopy (MFM). A MFM tip's effective magnetic charge,  $q$ , and effective magnetic moment along the tip's long axis,  $m_z$ , can be determined from the MFM signal of the ring at a different scan height and a different electric current in the ring. The magnetic moments in the directions transverse to the tip's long axis were estimated by a straight current wire. It was found that for a Si tip coated with 65 nm cobalt on one side,  $q$  is  $2.8 \times 10^{-6}$  emu/cm,  $m_z$  is  $3.8 \times 10^{-9}$  emu, and  $m_x$  and  $m_y$  are in the order of  $10^{-13}$  emu, which are negligible compared with  $m_z$ . Furthermore, the MFMs sensitivity to the second derivative of the magnetic field was determined from the minimum ring current for a measurable MFM signal to be 0.1 Oe/nm<sup>2</sup>.  
© 1997 American Institute of Physics. [S0003-6951(97)03115-X]

Magnetic force microscopy (MFM) is an essential tool for characterizing magnetic materials in submicron scale. However, to quantitatively interpret the MFM signal is very challenging, since the exact magnetic properties of a MFM tip are generally unknown. A number of methods have been used to quantify the MFM tip.<sup>1-5</sup> For examples, the hard magnetic disks and magnetic bacterium were used as calibration standards.<sup>2,5</sup> But the calibration was very crude, since the fields of the standards themselves cannot be determined exactly and can be altered, during the calibration, by the magnetic interaction between the tip and the standards. The hysteresis loops for various MFM tips were determined by using a straight current wire,<sup>6</sup> but this approach is not accurate in determining the magnetic moment in the tip axis (i.e.,  $m_z$ ), which is believed to play a dominant role in the MFM response.

It has been suggested that a MFM tip and hence MFM measurements can be quantified by using a micronscale ring.<sup>7</sup> Here, we report on the detailed experimental study and analysis of MFM calibration using micronscale current rings.

The metal rings were fabricated using electron-beam lithography and a lift-off technique.<sup>8,9</sup> In the fabrication, a resist, polymethyl methacrylate (PMMA), was first spun onto a SiO<sub>2</sub> substrate. Patterns of rings were exposed in the PMMA using a high resolution electron-beam lithography system. The exposed PMMA was removed during the development, leaving ring-shaped trenches in the PMMA. The 10 nm/120-nm-thick Ti/Au layers were evaporated into these ring-shaped trenches as well as on the top of the PMMA template. Finally, the PMMA was dissolved in acetone, lifting off the Au and Ti on top of the PMMA and leaving the rings on the SiO<sub>2</sub> substrate. The rings have an inner diameter of 1 or 5  $\mu\text{m}$  and a width of 200 nm. Scanning electron microscope (SEM) images of rings are shown in Fig. 1. A current supplied by a precision current source passed through the ring via two wire leads. The atomic force image and magnetic force image of the ring were measured simultaneously using a commercial magnetic force microscopy,

which was operated in TappingMode. The MFM tip used was made in house and has a 65-nm-thick Co film on only one side of a silicon tip, and was magnetized along the tip long axis,  $z$ , before the measurement.

Before describing our experimental results, we would like to discuss the principle of calibrating MFM in our experiment. For simplicity, we use a model which has only monopole and dipole interactions to describe the MFM tip. When the frequency that drives a MFM tip is kept constant, the phase shift in the tip vibration due to the force between the sample stray field and the MFM tip may be expressed as<sup>10,11</sup>

$$\Delta\Phi = \frac{Q}{k} \left( q \frac{\partial H_z}{\partial z} + m_x \frac{\partial^2 H_x}{\partial z^2} + m_y \frac{\partial^2 H_y}{\partial z^2} + m_z \frac{\partial^2 H_z}{\partial z^2} \right), \quad (1)$$

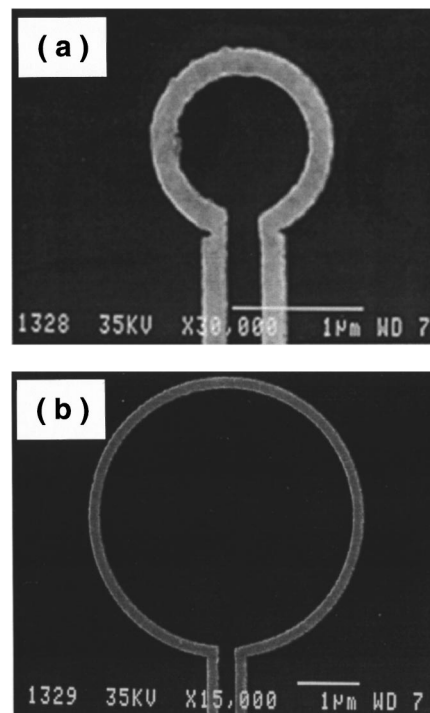


FIG. 1. SEM images of rings with an inner diameter of (a) 1 and (b) 5  $\mu\text{m}$ .

<sup>a)</sup>Electronic mail: lkong@ee.umn.edu

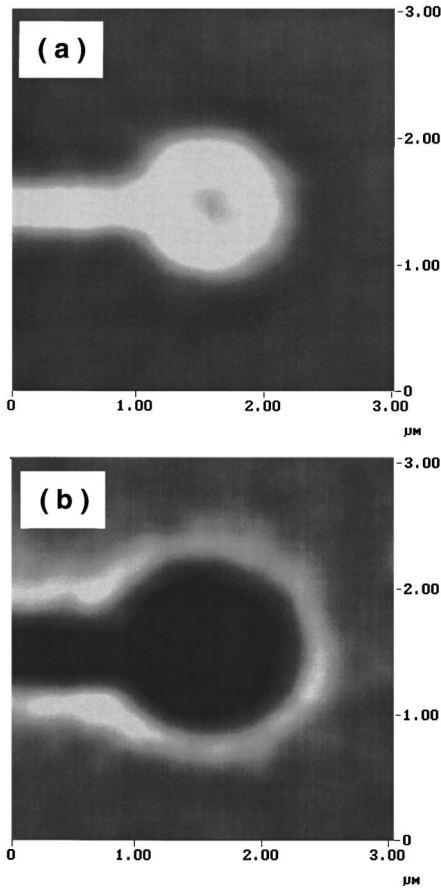


FIG. 2. MFM image of the same ring shown in Fig. 1 (a) when current  $I = \pm 2.5$  mA. The background is zero magnetic force and the dark area represents attractive magnetic force. (a) The field direction from the ring is opposite from the tip magnetization direction, and (b) the field direction is the same as the tip moment direction.

where  $Q$  is the quality factor of the MFM tip cantilever resonance,  $k$  is the spring constant of cantilever,  $q$  is the effective magnetic charge of the MFM tip,  $m_i$  ( $i=x, y,$  and  $z$ ) is the effective moment of the tip, and  $H_z$  is the vertical component of the sample stray field.

At the center of a current ring, the magnetic field has only the vertical component, and its value at height  $z$  above the ring center is given by

$$H_z = \frac{R^2}{2(z^2 + R^2)^{3/2}} I, \quad (2)$$

where  $R$  is the half diameter of the ring and  $I$  is the current in the ring. Therefore,

$$\frac{\partial H_z}{\partial z} = -\frac{3}{2} R^2 \frac{z}{(z^2 + R^2)^{5/2}} I, \quad (3)$$

$$\frac{\partial^2 H_z}{\partial z^2} = -\frac{3}{2} R^2 \left[ \frac{R^2 - 4z^2}{(z^2 + R^2)^{7/2}} \right] I. \quad (4)$$

In this case, Eq. (1) becomes

$$\Delta \Phi = -\frac{3R^2 Q}{2k} \left[ \frac{qz}{(z^2 + R^2)^{5/2}} + \frac{m_z(R^2 - 4z^2)}{(z^2 + R^2)^{7/2}} \right] I. \quad (5)$$

Using Eq. (5), we can estimate the tip effective magnetic charge  $q$  and the effective magnetic moment  $m_z$ , if we know

$Q$  and  $k$ . The quality factor  $Q$  can be determined by measuring the tip's resonance frequency,  $f_0$ , and the full bandwidth,  $\Delta f_0$ , at 0.707 of the maximum amplitude:<sup>12</sup>

$$Q = \frac{f_0}{\Delta f_0}. \quad (6)$$

The tip's spring constant  $k$  can be calculated from<sup>13</sup>

$$k = \frac{\rho l w t f_0^2}{0.105}, \quad (7)$$

where  $t$ ,  $w$ , and  $l$  are the thickness, width, and length of the cantilever for the MFM probe, respectively, which can be determined using SEM, and  $\rho$  is the density of the cantilever.

Figure 2(a) and 2(b) show the MFM image of the ring with an inner diameter of  $1 \mu\text{m}$  when  $I = \pm 2.5$  mA, respectively. The MFM signal polarity depended on the current direction, and was inverted when the current direction was reversed.

Figure 3 shows the MFM signal of the tip with 65-nm-thick Co film, at the center of the  $5 \mu\text{m}$  diameter current ring with a 5 mA current, as the function of the distance between the tip and the ring. Without knowing  $k$  and  $Q$  of the MFM tip, the fitting of the data in Fig. 3 into Eq. (5) gives the ratio of the effective magnetic moment and the effective magnetic charge,  $m_z/q = 11 \mu\text{m}$ .

It can be found from the above ratio that the dipole interaction is about two orders of magnitude larger than the monopole interaction when the tip-ring separation is from 0 to  $0.1 \mu\text{m}$ . Therefore, we can neglect the monopole interaction and determine  $m_z$  using the response signal of the MFM at the ring center as a function of the current in the ring, shown in Fig. 4. The signal varies nearly linearly with the current, which is consistent with Eq. (5), suggesting that the MFM tip magnetization stays constant when the magnetic field from the ring increases.

The  $f_0$  and  $\Delta f_0$  of the tip were determined to be 60.8 and 0.39 kHz, respectively. From Eq. (6), we obtained the quality factor  $Q = 156$ . From Eq. (7), we obtained the spring constant  $k = 24$  N/m by putting  $t = 3.4 \mu\text{m}$ ,  $w = 37 \mu\text{m}$ , length  $l = 240 \mu\text{m}$ , which were determined from the SEM image of the cantilever of the MFM probe, and  $\rho = 2.33 \text{ g/cm}^3$  for Si. So the effective magnetic moment of the tip,  $m_z$ , is

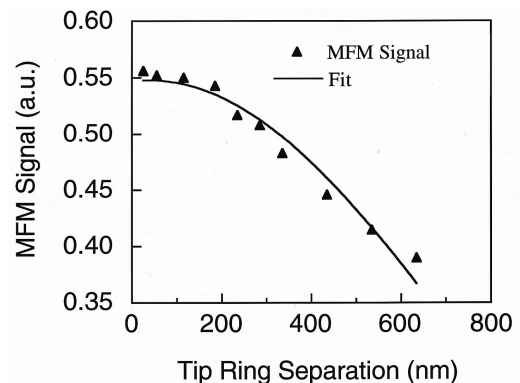


FIG. 3. MFM signal at the ring center vs the tip-ring separation for the ring with an inner diameter of  $5 \mu\text{m}$  and a current of 5 mA using the tip with 65-nm-thick Co film. The triangles represent the experimental data and the solid line is the fitting result using Eq. (5).

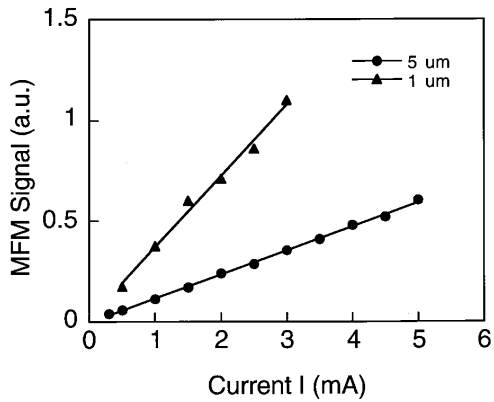


FIG. 4. Phase shift  $\Delta\phi$  of MFM vs current  $I$  in the ring with an inner diameter of 1 and 5  $\mu\text{m}$  using the tip with 65-nm-thick Co film, showing a nearly linear relation.

$3.8 \times 10^{-9}$  emu. Using  $m_z/q = 11 \mu\text{m}$  obtained from Fig. 3, we get the effective magnetic charge,  $q$ , of  $2.8 \times 10^{-6}$  emu/cm. The measured dipole moment is very close to the value estimated from the Co film deposited on the tip if the Co film is polarized like a dipole.

The other two components of the tip effective moment  $m_x$  and  $m_y$  were determined using tip to scan along and across a straight current wire. Both  $m_x$  and  $m_y$  were found to be in the order of  $10^{-13}$  emu, about four orders smaller than  $m_z$ , indicating that  $m_x$  and  $m_y$  of the tip can be neglected compared to  $m_z$ .

Now let us discuss other issues in the calibration of MFM tips. First, the ring with a 5  $\mu\text{m}$  diameter is better than a 1  $\mu\text{m}$  diameter ring for the MFM calibration because of two things: (a) the observable MFM signal has a larger range of scan height; (b) as shown in Fig. 5, for a given scanning height, the MFM signal is almost constant over a larger area around the ring center, making the calibration less sensitive to the  $x$ - $y$  position accuracy. Second, the significance of the magnetic charge and the dipole in MFM signal depends on the scan height. In Fig. 3, when the tip-ring separation is from 0 to 0.1  $\mu\text{m}$ , the dipole interaction is about two orders larger than the monopole interaction, therefore the monopole interaction can almost be neglected. Third, note that in Fig. 4 when the current was less than 0.2 mA, no MFM signal but only noise was observed, which gives the measurement sensitivity of the MFM system (i.e., the minimum second derivative of the magnetic field that our tip can measure) of 0.1 Oe/nm<sup>2</sup>. Fourth, when using a current ring with an inner diameter of 1  $\mu\text{m}$  to characterize the same tip, we found that the  $m_z$  value is about one order smaller than that obtained from the 5  $\mu\text{m}$  diameter ring. This is because in part that as the ring size becomes comparable to the MFM tip size, the equations described previously must be modified significantly. Finally, to reduce the MFM tip size effect and to achieve a high resolution measurement, the spike MFM tip should be used.<sup>14</sup>

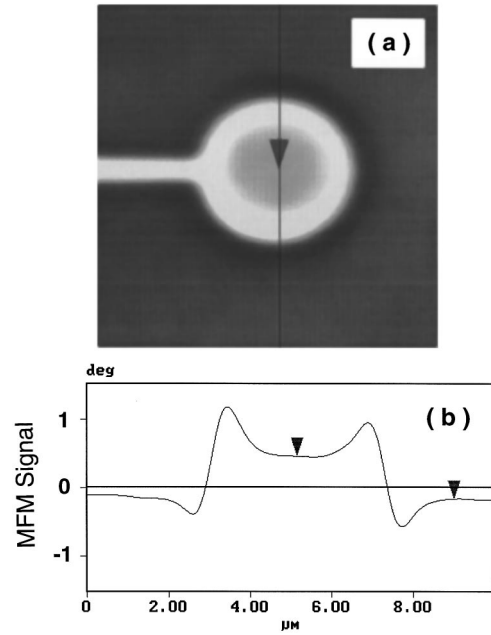


FIG. 5. (a) MFM image of the ring with an inner diameter of 5  $\mu\text{m}$  using the tip with 65-nm-thick Co film when the current was 5 mA and the scan height was 90 nm; (b) MFM signal along the black line in (a).

In conclusion, we have shown that micronscale current rings can quantify the MFM signal, the effective magnetic charge and magnetic moment of a MFM tip, and the MFMs sensitivity.

The authors would like to thank P. R. Krauss and B. Guibord for assistance in fabrication. This work was partially supported by DARPA through ONR, Contract No. N00014-93-1-0648 and ONR, Contract No. N00014-93-0256.

- <sup>1</sup>D. Rugar, H. J. Mamin, P. Guethner, S. E. Lambert, J. E. Stern, I. McFadyen, and T. Yogi, *J. Appl. Phys.* **68**, 1169 (1990).
- <sup>2</sup>K. Babcock, V. Elings, M. Dugas, and S. Loper, *IEEE Trans. Magn.* **30**, 4503 (1994).
- <sup>3</sup>R. B. Proksch, S. Foss, and E. D. Dahlberg, *IEEE Trans. Magn.* **30**, 4467 (1994).
- <sup>4</sup>T. Goddenhenrich, H. Lemke, M. Muck, U. Hartmann, and C. Heiden, *Appl. Phys. Lett.* **57**, 2612 (1990).
- <sup>5</sup>R. B. Proksch, T. E. Schaffer, B. M. Moskowitz, E. D. Dahlberg, D. A. Bazylinski, and R. B. Frankel, *Appl. Phys. Lett.* **66**, 2582 (1995).
- <sup>6</sup>K. L. Babcock, V. B. Elings, J. Shi, D. D. Awschalom, and M. Dugas, *Appl. Phys. Lett.* **69**, 705 (1996).
- <sup>7</sup>S. Y. Chou (private communication).
- <sup>8</sup>P. B. Fischer and S. Y. Chou, *Appl. Phys. Lett.* **62**, 2989 (1993).
- <sup>9</sup>P. B. Fischer, K. Dai, E. Chen, and S. Y. Chou, *J. Vac. Sci. Technol. B* **11**, 2524 (1993).
- <sup>10</sup>K. Babcock, M. Dugas, S. Manalis, and V. Elings, *Mater. Res. Soc. Symp. Proc.* **355**, 311 (1995).
- <sup>11</sup>P. Grütter, H. J. Mamin, and D. Rugar, in *Scanning Tunneling Microscopy II*, edited by R. Weisendanger and H.-J. Güntherodt (Springer, Berlin, 1992), pp. 151–207.
- <sup>12</sup>D. Sarid, in *Scanner Force Microscopy*, edited by M. Lapp and H. Stark (Oxford University Press, New York, 1991), p. 21.
- <sup>13</sup>O. Wolter, Th. Bayer, and J. Greschner, *J. Vac. Sci. Technol. B* **9**, 1353 (1991).
- <sup>14</sup>P. B. Fischer, M. S. Wei, and S. Y. Chou, *J. Vac. Sci. Technol. B* **11**, 2570 (1993).